JOURNAL OF SYNCHROTRON RADIATION

ISSN: 1600-5775
journals.iucr.org/s

Pressure effects on the EXAFS Debye–Waller factor of iron

Ho Khac Hieu, Nguyen Ba Duc, Nguyen Van Hung, Pham Thi Minh Hanh and Tran Thi Hai

J. Synchrotron Rad. (2020). **27**, 1372–1375

JOURNAL OF SYNCHROTRON RADIATION

ISSN 1600-5775

Received 20 March 2020
Accepted 16 July 2020

Edited by G. Grübel, HASYLAB at DESY, Germany

Keywords: Debye model; EXAFS; Debye–Waller factor; Debye frequency.

Pressure effects on the EXAFS Debye–Waller factor of iron

Ho Khac Hieu,[a,b]* Nguyen Ba Duc,[c] Nguyen Van Hung,[d] Pham Thi Minh Hanh[e] and Tran Thi Hai[f]

[a]Institute of Research and Development, Duy Tan University, 03 Quang Trung, Hai Chau, Da Nang 550000, Vietnam, [b]Faculty of Natural Sciences, Duy Tan University, 03 Quang Trung, Hai Chau, Da Nang 550000, Vietnam, [c]Tan Trao University, Km 6, Yen Son, Tuyen Quang 301910, Vietnam, [d]VNU University of Science, 334 Nguyen Trai, Thanh Xuan, Ha Noi 100000, Vietnam, [e]Hanoi Pedagogical University No 2, Vinh Phuc 280000, Vietnam, and [f]Hong Duc University, 565 Quang Trung, Dong Ve, Thanh Hoa 441430, Vietnam. *Correspondence e-mail: hieuhk@duytan.edu.vn

The pressure effects on atomic mean-square relative displacement characterizing the extended X-ray absorption fine structure (EXAFS) Debye–Waller factor of iron metal have been investigated based on the Debye model. The analytical expressions of the Debye frequency and EXAFS Debye–Waller factor have been derived as functions of crystal volume compressibility. Based on the well established equation-of-state including the contributions of the anharmonic and electronic thermal pressures, numerical calculations have been performed for iron up to a pressure of 220 GPa and compared with experimental data when possible. These results show that the Debye frequency increases rapidly with compression, and beyond 150 GPa it behaves as a linear function of pressure. Meanwhile the mean-square relative displacement curve drops robustly with pressure, especially at pressures smaller than 100 GPa. This phenomenon causes the enhancement of EXAFS signals at high pressure. Reversely, the increasing of temperature will reduce the amplitude of EXAFS spectra.

1. Introduction

Iron is a main component in the Earth's core. The high-pressure thermodynamic properties of iron are primarily important information for explaining geochemical observations and seismic data, and for modeling the dynamic properties, evolution process, structure and dynamo of the Earth. A number of theoretical and experimental works have been performed to study the structure and thermodynamic properties of iron at extreme conditions, such as first-principles calculations (Stixrude, 2012), molecular dynamics simulations (Alfè, 2010), laser-heated diamond-anvil cells (DACs) (Errandonea, 2013), shock-wave experiments (Nguyen & Holmes, 2004) and X-ray absorption spectroscopy (Wang & Ingalls, 1998; Ishimatsu *et al.*, 2016; Torchio *et al.*, 2016).

Extended X-ray absorption fine-structure spectroscopy (EXAFS) (Crozier *et al.*, 1988) is a powerful method for investigation of local structure and thermodynamic properties of materials. It is a result of the interference between outgoing photoelectron waves and back-scattering due to the presence of neighboring atoms. The Debye–Waller factor (DWF) $W(k) = \exp(-2\sigma^2 k^2)$ (where k is the wavenumber and σ^2 is the second EXAFS cumulant) is one important factor of the EXAFS oscillation function. The second EXAFS cumulant σ^2 or EXAFS DWF accounts for the effects of atomic thermal vibrations and influences sensitively the EXAFS amplitudes. Previously, compression effects on the EXAFS DWF have been considered in some theoretical approaches (Hung *et al.*,

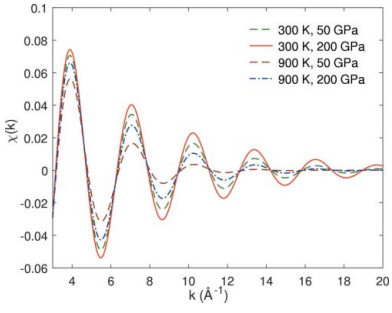

2011; Hieu & Hung, 2013). Using dynamic compression with multiple shocks, EXAFS measurements on the compressed iron were performed up to 560 GPa by taking into account anharmonic effects (Ping *et al.*, 2013). In spite of this, there is still no complete theory that allows us to theoretically predict the EXAFS parameters at high pressure.

In this work, we investigate the pressure effects on the Debye frequency and EXAFS DWF of iron metal based on the Debye model. Numerical calculations are performed up to a pressure of 220 GPa and compared with those of previous works when possible.

2. Theoretical approach

The Debye–Waller factor $W(k) = \exp(-2\sigma^2 k^2)$ accounts for the effects of atomic thermal vibrations in EXAFS. The second EXAFS cumulant σ^2 characterizes the variance of the distance distribution corresponding to the parallel mean-square relative displacement (MSRD) of the bond between absorber and backscatterer atoms. Hung *et al.* (2010), using the anharmonic correlated Debye model, derived an expression for the EXAFS DWF as a function of temperature T as

$$\sigma^2(T) = -\frac{2\hbar a}{\pi M \omega_{\rm D}^2} \int_0^{\pi/a} \frac{1+z(q)}{1-z(q)}\, \omega(q)\, {\rm d}q, \qquad (1)$$

where a is the lattice constant, q is the phonon wavenumber, M is the mass of composite atoms, $z(q) = \exp[\hbar\omega(q)/k_{\rm B}T]$, $k_{\rm B}$ is the Boltzmann constant and $\omega(q)$ is the dispersion relation which achieves the maximum value of the Debye frequency $\omega_{\rm D}$ at the boundaries $q = \pm\pi/a$ of the first Brillouin zone of the linear chain. The phonon frequency $\omega(q)$ is expressed as (Hung *et al.*, 2010)

$$\omega(q) = \omega_{\rm D} \left|\sin\left(\frac{qa}{2}\right)\right|, \qquad |q| \le \pi/a. \qquad (2)$$

From equation (1), the pressure effects on the MSRD can be investigated indirectly through the evaluation of lattice parameter a and the Debye frequency $\omega_{\rm D}$ under compression. The volume-dependent lattice parameter can be determined as $a = a_0\zeta^{1/3}$, where ζ is the volume compression ratio $\zeta = V/V_0$ (V is the volume of the crystal; a_0 and V_0 are values of a and V at ambient conditions). Meanwhile the volume dependence of the Debye frequency can be considered through the Grüneisen parameter $\gamma_{\rm G}$ as (Hieu, 2015)

$$\gamma_{\rm G} = -\frac{\partial \ln \omega_{\rm D}}{\partial \ln V}. \qquad (3)$$

Previous works (Boehler, 1983; Hieu, 2014) showed that at low pressure the Grüneisen parameter reduces gradually when pressure increases. A simple power-law form of the volume-dependent Grüneisen parameter suggested by Graf *et al.* (2004) is $\gamma_{\rm G} = \gamma_0\zeta^p$, where $p > 0$ is a material constant, and γ_0 is the Grüneisen parameter at ambient conditions (Errandonea, 2013; Hieu & Ha, 2013). However, this power law does not describe well the Grüneisen parameter of materials at high compression. Another well described form of the Grüneisen parameter following the Al'tshuler *et al.* (1987) proposition has been chosen as (Dewaele *et al.*, 2006)

$$\gamma_{\rm G} = \gamma_\infty + (\gamma_0 - \gamma_\infty)\,\zeta^\beta \quad \text{with} \quad \beta = \frac{\gamma_0}{\gamma_0 - \gamma_\infty}, \qquad (4)$$

where γ_∞ is the value of the Grüneisen parameter $\gamma_{\rm G}$ at infinite compression.

By substituting equation (4) into equation (3) and taking the integral, we find the Debye frequency as a function of volume compression $\zeta = V/V_0$ as

$$\omega_{\rm D}(\zeta) = \omega_0\, \zeta^{-\gamma_\infty} \exp\left[-\frac{\gamma_0}{\beta^2}\left(\zeta^\beta - 1\right)\right], \qquad (5)$$

where ω_0 is the value of the Debye frequency of iron at ambient conditions. This quantity can be measured from experiments or calculated from the correlated Debye model (Sevillano *et al.*, 1979).

By substituting equations (5) and (2) into equation (1), we finally derive the volume-dependent MSRD expression as

$$\sigma^2(\zeta, T) = -\frac{2\hbar a \zeta^{\gamma_\infty}}{\pi M \omega_0} \exp\left[\frac{\gamma_0}{\beta^2}\left(\zeta^\beta - 1\right)\right] \times \int_0^{\pi/a} \frac{1+z(\zeta,q)}{1-z(\zeta,q)} \left|\sin\left(\frac{qa}{2}\right)\right| {\rm d}q. \qquad (6)$$

In order to study the pressure effects on the Debye frequency and atomic MSRD of iron, we need an accurate equation-of-state (EOS) relating the pressure–volume–temperature of the system. In the work of Dewaele *et al.* (2006), based on the DAC experiments, combined with X-ray diffraction, Hugoniot data and *ab initio* modeling, a high-pressure high-temperature quasi-hydrostatic EOS of h.c.p.-iron was constructed as

$$P(V, T) = P_V(V,\ 300\ {\rm K}) + \left[P_{\rm TH}(V, T) - P_{\rm TH}(V,\ 300\ {\rm K})\right], \qquad (7)$$

where $P_V(V, 300\ {\rm K})$ is the isothermal (cold) pressure at temperature 300 K and $P_{\rm TH}(V, T)$ is the temperature-dependent (thermal) pressure. These two pressures, $P_V(V, 300\ {\rm K})$ and $P_{\rm TH}(V, T)$, are expressed, using the fitted Vinet EOS (Anderson, 1995) and the formalism derived by Dorogokupets & Oganov (2007), by equations (8) and (9), respectively, as

$$P_V(V, 300\ {\rm K}) = 3B_0\zeta^{-2/3}\left(1-\zeta^{1/3}\right) \times \exp\left[\frac{3}{2}\left(B_0' - 1\right)\left(1-\zeta^{1/3}\right)\right], \qquad (8)$$

$$P_{\rm TH}(V, T) = \frac{9R\gamma_{\rm G}}{V}\left[\frac{\theta_{\rm D}}{8} + T\left(\frac{T}{\theta_{\rm D}}\right)^3 \int_0^{\theta_{\rm D}/T} \frac{y^3\, {\rm d}y}{e^y - 1}\right] + \frac{3R}{2V}\left(b_0\, m\, \zeta^m + e_0\, n\, \zeta^n\right)T^2, \qquad (9)$$

where B_0 and B_0' are the isothermal bulk modulus and its first-pressure derivative, respectively; R denotes the gas constant. The first term of the right-hand side of equation (9) represents the main part of $P_{\rm TH}$, which is the quasi-harmonic Debye thermal pressure (Anderson, 1995). The second term includes

the contributions of the anharmonic and electronic thermal pressure (Alfè *et al.*, 2001).

3. Results and discussion

In this section, numerical calculations are performed for iron up to 220 GPa. Here it should be noted that experimental evidence shows an h.c.p.–b.c.c. transition line in pressure–temperature space from about 95 ± 2 GPa and 2986 ± 79 K to at least 222 ± 6 GPa and 4192 ± 104 K (Hrubiak *et al.*, 2018). The parameters b_0, e_0, m and n of equation (7) have been derived for iron by fitting first-principles anharmonic and electronic thermal pressures as (Dewaele *et al.*, 2006) b_0 = 3.7×10^{-5} K^{-1}, $e_0 = 1.95 \times 10^{-4}$ K^{-1}, $m = 1.87$ and $n = 1.339$. The fitted values of γ_0 and γ_∞ are 1.710 and 1.305, respectively. The Debye temperature θ_0 at ambient conditions is fixed as 417 K (the Debye frequency $\omega_0 = k_B\theta_0/\hbar$ = 5.46×10^{13} Hz), the isothermal bulk modulus B_0 and its first-pressure derivative B_0' are 163.4 GPa and 5.38, respectively (Dewaele *et al.*, 2006).

In Fig. 1, we show the pressure dependence of the Debye frequency of iron up to 220 GPa. Experimental results of Wang & Ingalls (1998) and Anderson *et al.* (2001) have also been presented for comparison. Anderson *et al.* (2001) have extracted this thermodynamic quantity from the atomic mean-square displacement which was obtained by X-ray structural refinement using the Rietveld method on powder diffraction measurements. As can be observed from Fig. 1, our theoretical calculation follows the experimental data (Wang & Ingalls, 1998; Anderson *et al.*, 2001) up to a pressure of about 200 GPa. Beyond 150 GPa, the slope of the Debye frequency curve becomes reducible and it is almost linear proportional to pressure. The initial slope of this curve is about 4.4 K GPa^{-1}, but, from a pressure of 150 GPa and beyond, the average slope is about 1.2 K GPa^{-1}.

Using the derived Debye frequency ω_D, we can investigate the pressure effects on the parallel MSRD of iron. The pressure dependence of the atomic MSRD characterizing the EXAFS DWF of iron metal at different temperatures (T = 300 K, 500 K, 700 K, 900 K) is shown in Fig. 2. From this figure we can see that the MSRD curves of iron drop rapidly (especially at pressures smaller than 100 GPa). This phenomenon forecasts the enhancement of EXAFS signals at high pressure. Above 200 GPa, atomic MSRD curves are readily seen to be in approximately linear proportion to pressure. The initial slopes of MSRD curves $d\sigma^2/dP$ at ambient pressure are -1.12×10^{-4}, -1.88×10^{-4}, -2.63×10^{-4} and -3.39×10^{-4} Å^2 GPa^{-1} corresponding to temperatures of 300, 500, 700 and 900 K. Meanwhile, the slopes of MSRD curves at temperature 300 K, 500 K, 700 K and 900 K and at pressure 200 GPa are -4.87×10^{-6}, -8.23×10^{-6}, -1.17×10^{-5} and -1.52×10^{-5} Å^2 GPa^{-1}, respectively. Due to the lack of available experimental data and theoretical calculations, the comparison for pressure-dependent MSRD of iron has been neglected.

Our calculations predict that the Debye frequency increases robustly with pressure, while the EXAFS DWF of iron drops rapidly. The rise of the phonon frequency and the reduction of atomic MSRD can be explained by the constraint of atomic vibrations due to the increasing of compression. It is worth mentioning that the EXAFS DWF is susceptible to both static disorder and thermal disorder. The first one represents the structural disorder caused by alloying or strain while the second one represents the disorder due to the thermal vibrations of atoms. The latter gives us the information of the bond-stretching force constant between absorber and backscatterer atoms coming close to the dynamic properties of them (Hong *et al.*, 2019). As can be realized from Fig. 2, the EXAFS DWF enhances robustly when increasing the temperature. This behavior of atomic MSRD is palpable evidence for significant contribution of thermal disorder in the high-temperature region.

Using the derived EXAFS DWF, we calculate the theoretical EXAFS spectra of iron at temperatures 300 K and 900 K, and at pressures 50 GPa and 200 GPa. These four calculated EXAFS curves are shown in Fig. 3. Here it should be noted that, for simplicity, we have neglected the pressure-induced

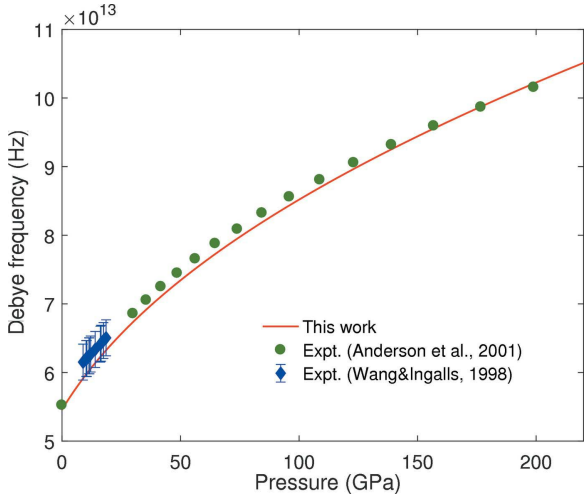

Figure 1
Pressure-dependent Debye frequency of iron.

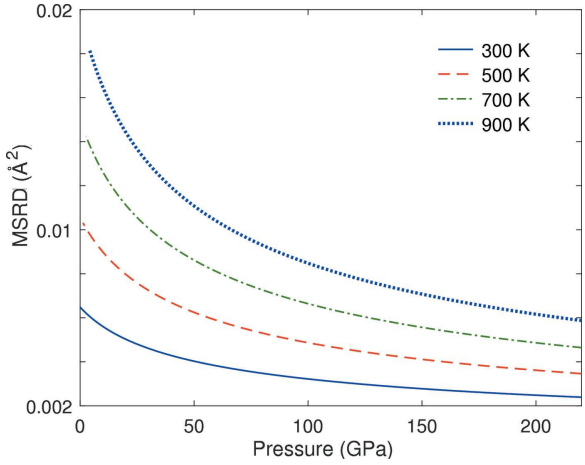

Figure 2
Pressure dependence of MSRD of iron at 300 K, 500 K, 700 K and 900 K.

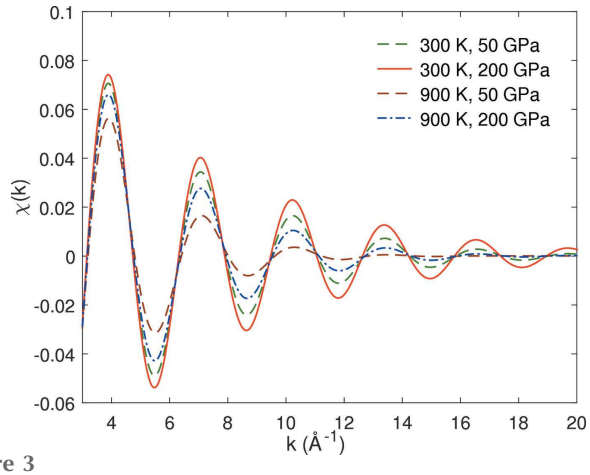

Figure 3
Theoretical prediction of EXAFS signals of iron at pressure 50 GPa and 200 GPa, and at two different temperatures 300 K and 900 K.

and temperature-induced phase shift of EXAFS spectroscopy caused by the variation of temperature and pressure. As can be clearly observed from this figure, at a fixed pressure, increasing the temperature will reduce the amplitude of EXAFS spectra. Reversely, at a specified temperature, an increasing of pressure will intensify the EXAFS signals.

4. Conclusions

In conclusion, the Debye model has been developed to investigate the pressure dependence of the EXAFS DWF of iron based on the volume-dependent Grüneisen parameter. We derived the analytical expressions of the Debye frequency and parallel MSRD as functions of volume compression. Numerical calculations for iron up to a pressure of 220 GPa show that the Debye frequency increases rapidly with compression, and beyond 150 GPa it behaves like a linear function of pressure. Meanwhile, the MSRD curve drops robustly with pressure, especially at pressures smaller than 100 GPa. The decreasing of MSRD of iron causes the enhancement of EXAFS signals at high pressure. In contrast, the increasing of temperature will fall off the EXAFS spectra. This work can be seen as a useful reference for future experimental measurements of high-pressure MSRD factors of materials.

Acknowledgements

The authors would like to acknowledge Professor Anatoly Belonoshko and an anonymous reviewer for their useful comments and suggestions.

Funding information

Funding for this research was provided by: the Vietnam National Foundation for Science and Technology Development (NAFOSTED) under grant number 103.01-2017.343 (to Hieu Ho).

References

Alfè, D. (2010). *Rev. Mineral. Geochem.* **71**, 337–354.
Alfè, D., Price, G. D. & Gillan, M. J. (2001). *Phys. Rev. B*, **64**, 045123.
Al'tshuler, L. V., Brusnikin, S. E. & Kuz'menkov, E. A. (1987). *J Appl. Mech. Tech. Phys.* **28**, 129–141.
Anderson, L., Dubrovinsky, L., Saxena, S. K. & LeBihan, T. (2001). *Geophys. Res. Lett.* **28**, 399–402.
Anderson, O. L. (1995). *Equations of State for Solids in Geophysics and Ceramic Science, Oxford Monographs on Geology and Geogphysics.* Oxford University Press.
Boehler, R. (1983). *Phys. Rev. B*, **27**, 6754–6762.
Crozier, E. D., Rehr, J. J. & Ingalls, R. (1988). *X-ray Absorption: Principles, Applications, Techniques of EXAFS, SEXAFS and XANES*, 1st ed., edited by D. C. Koningsberger and R. Prins. Wiley-Interscience.
Dewaele, P., Loubeyre, F., Occelli, M., Mezouar, M., Dorogokupets, P. I. & Torrent, M. (2006). *Phys. Rev. Lett.* **97**, 215504.
Dorogokupets, P. I. & Oganov, A. R. (2007). *Phys. Rev. B*, **75**, 024115.
Errandonea, D. (2013). *Phys. Rev. B*, **87**, 054108.
Graf, M. J., Gree, C. W. & Boettger, J. C. (2004). *AIP Conf. Proc.* **706**, 65–68.
Hieu, H. K. (2014). *Vacuum*, **109**, 184–186.
Hieu, H. K. (2015). *Vacuum*, **120**, 13–16.
Hieu, H. K. & Ha, N. N. (2013). *AIP Adv.* **3**, 112125.
Hieu, H. K. & Hung, V. V. (2013). *High. Press. Res.* **33**, 768–776.
Hong, N. T., Hieu, H. K., Duc, N. B., Phuong, D. D., Tuyen, N. V. & Khoa, D. Q. (2019). *Vacuum*, **163**, 210–215.
Hrubiak, R., Meng, Y. & Shen, G. (2018). *arXiv*:1804.05109 [physics. geo-ph].
Hung, N. B., Bao Trung, N. & Kirchner, B. (2010). *Physica B*, **405**, 2519–2525.
Hung, N. V., Hung, H. K., Hieu, H. K. & Frahm, R. R. (2011). *Physica B*, **406**, 456–460.
Ishimatsu, N., Kawamura, M., Mizumaki, H., Maruyama, H., Sumiya, H. & Irifune, T. (2016). *High. Press. Res.* **36**, 381–390.
Nguyen, J. H. & Holmes, N. C. (2004). *Nature*, **427**, 339–342.
Ping, F., Coppari, F., Hicks, B., Yaakobi, B., Fratanduono, S., Hamel, S., Eggert, J. R., Rygg, R. F., Smith, D. C., Swift, D. G., Braun, T. R., Boehly, T. R. & Collins, G. W. (2013). *Phys. Rev. Lett.* **111**, 065501.
Sevillano, H., Meuth, H. & Rehr, J. J. (1979). *Phys. Rev. B*, **20**, 4908–4911.
Stixrude, L. (2012). *Phys. Rev. Lett.* **108**, 055505.
Torchio, F., Occelli, O., Mathon, A., Sollier, E., Lescoute, L., Videau, T., Vinci, A., Benuzzi-Mounaix, J., Headspith, W., Helsby, S., Bland, D., Eakins, D., Chapman, S., Pascarelli, S. & Loubeyre, P. (2016). *Sci. Rep.* **6**, 26402.
Wang, F. M. & Ingalls, R. (1998). *Phys. Rev. B*, **57**, 5647–5654.